Estimating modal instability threshold for photonic crystal rod fiber amplifiers

Johansen, Mette Marie; Hansen, Kristian Rymann; Laurila, Marko; Alkeskjold, Thomas Tanggaard; Lægsgaard, Jesper

Published in:
Optics Express

Link to article, DOI:
10.1364/OE.21.015409

Publication date:
2013

Document Version
Publisher's PDF, also known as Version of record

Estimating modal instability threshold for photonic crystal rod fiber amplifiers

Mette Marie Johansen,[1*] Kristian Rymann Hansen,[1] Marko Laurila,[2] Thomas Tanggaard Alkeskjold,[2] and Jesper Lægsgaard[1]

[1]*DTU Fotonik, Technical University of Denmark, Ørsteds Plads building 343, 2800 Kgs. Lyngby, DK-Denmark*
[2]*NKT Photonics A/S, Blokken 84, 3460 Birkerød, DK-Denmark*
[*]*mmajo@fotonik.dtu.dk*

Abstract: We present a semi-analytic numerical model to estimate the transverse modal instability (TMI) threshold for photonic crystal rod amplifiers. The model includes thermally induced waveguide perturbations in the fiber cross section modeled with finite element simulations, and the relative intensity noise (RIN) of the seed laser, which seeds mode coupling between the fundamental and higher order mode. The TMI threshold is predicted to ~370 W – 440 W depending on RIN for the distributed modal filtering rod fiber.

OCIS codes: (060.2280) Fiber design and fabrication; (060.2320) Fiber optics ampli□ers and oscillators; (060.4005) Micro structured fibers; (140.6810) Thermal effects.

References and links

1. D. J. Richardson, J. Nilsson, and W. A. Clarkson, "High power fiber lasers: current status and future perspectives [Invited]," J. Opt. Soc. Am. B **27**(11), B63–B92 (2010).
2. T. T. Alkeskjold, M. Laurila, L. Scolari, and J. Broeng, "Single-mode ytterbium-doped large-mode-area photonic bandgap rod fiber amplifier," Opt. Express **19**(8), 7398–7409 (2011).
3. F. Jansen, F. Stutzki, H.-J. Otto, M. Baumgartl, C. Jauregui, J. Limpert, and A. Tünnermann, "The influence of index-depressions in core-pumped Yb-doped large pitch fibers," Opt. Express **18**(26), 26834–26842 (2010).
4. A. V. Smith and J. J. Smith, "Mode instability in high power fiber amplifiers," Opt. Express **19**(11), 10180–10192 (2011).
5. T. Eidam, C. Wirth, C. Jauregui, F. Stutzki, F. Jansen, H.-J. Otto, O. Schmidt, T. Schreiber, J. Limpert, and A. Tünnermann, "Experimental observations of the threshold-like onset of mode instabilities in high power fiber amplifiers," Opt. Express **19**(14), 13218–13224 (2011).
6. B. Ward, C. Robin, and I. Dajani, "Origin of thermal modal instabilities in large mode area fiber amplifiers," Opt. Express **20**(10), 11407–11422 (2012).
7. C. Jauregui, T. Eidam, J. Limpert, and A. Tünnermann, "The impact of modal interference on the beam quality of high-power fiber amplifiers," Opt. Express **19**(4), 3258–3271 (2011).
8. K. R. Hansen, T. T. Alkeskjold, J. Broeng, and J. Lægsgaard, "Thermally induced mode coupling in rare-earth doped fiber amplifiers," Opt. Lett. **37**(12), 2382–2384 (2012).
9. K. R. Hansen, T. T. Alkeskjold, J. Broeng, and J. Lægsgaard, "Theoretical analysis of mode instability in high-power fiber amplifiers," Opt. Express **21**(2), 1944–1971 (2013).
10. E. Coscelli, F. Poli, T. T. Alkeskjold, M. M. Jørgensen, L. Leick, J. Broeng, A. Cucinotta, and S. Selleri, "Thermal Effects on the Single-Mode Regime of Distributed Modal Filtering Rod Fiber," J. Lightwave Technol. **30**(22), 3494–3499 (2012).
11. D. C. Brown and H. J. Hoffman, "Thermal, stress, and thermo-optic effects in high average power double-clad silica fiber lasers," J. Quant. Electron. **37**(2), 207–217 (2001).
12. M.-A. Lapointe, S. Chatigny, M. Piché, M. Cain-Skaff, and J.-N. Maran, "Thermal effects in high power cw fiber lasers," Proc. SPIE **7195**, 71951U, 71951U-11 (2009).
13. J. Limpert, T. Schreiber, A. Liem, S. Nolte, H. Zellmer, T. Peschel, V. Guyenot, and A. Tünnermann, "Thermo-optical properties of air-clad photonic crystal fiber lasers in high power operation," Opt. Express **11**(22), 2982–2990 (2003).
14. Comsol, "Products," <http://www.comsol.com/products/multiphysics/> (2 January 2013).
15. M. M. Jørgensen, S. R. Petersen, M. Laurila, J. Lægsgaard, and T. T. Alkeskjold, "Optimizing single mode robustness of the distributed modal filtering rod fiber amplifier," Opt. Express **20**(7), 7263–7273 (2012).
16. M. Laurila, M. M. Jørgensen, K. R. Hansen, T. T. Alkeskjold, J. Broeng, and J. Lægsgaard, "Distributed mode filtering rod fiber amplifier delivering 292W with improved mode stability," Opt. Express **20**(5), 5742–5753 (2012).
17. F. Stutzki, H.-J. Otto, F. Jansen, C. Gaida, C. Jauregui, J. Limpert, and A. Tünnermann, "High-speed modal decomposition of mode instabilities in high-power fiber lasers," Opt. Lett. **36**(23), 4572–4574 (2011).

#189034 - $15.00 USD Received 17 Apr 2013; revised 13 Jun 2013; accepted 13 Jun 2013; published 20 Jun 2013

18. H.-J. Otto, F. Stutzki, F. Jansen, T. Eidam, C. Jauregui, J. Limpert, and A. Tünnermann, "Temporal dynamics of mode instabilities in high-power fiber lasers and amplifiers," Opt. Express **20**(14), 15710–15722 (2012).
19. A. V. Smith and J. J. Smith, "Influence of pump and seed modulation on the mode instability thresholds of fiber amplifiers," Opt. Express **20**(22), 24545–24558 (2012).

1. Introduction

Rare-earth doped very large mode area (LMA) fiber amplifiers have gained increasing attention due to their high output powers with excellent beam quality and good pointing stability [1]. High pulse energies and peak powers require a large effective area, making it challenging to maintain single mode (SM) behavior. New complex fiber designs favor large differential gain between the fundamental mode (FM) and higher order mode (HOM); for instance by using resonant structures in the cladding to effectively remove HOMs from the core [2], or delocalizing HOMs at low signal powers [3]. Currently, the onset of transverse modal instability (TMI) degrading the output beam quality sets the upper limit for power scaling [4–6]. TMI sets in as the average signal power reaches a certain threshold, typically on the order of a few hundred W. A phase shift between a thermally induced index grating at high power levels and the signal causes power transfer from the FM to a HOM leading to TMI. Numerically heavy beam propagation models have been used to study temporal and spectral modal instability properties with impressive results gaining further insight into the phenomenon [4,6,7]. Recently, a numerically simpler model, by Hansen et *al.* [8], was published using a semi-analytic approach to consider thermally induced mode coupling by a coupled-mode model. In [9], the authors extended the model to include temporal and spectral evolution of TMI and successfully described fiber amplifier characteristics at and above TMI threshold.

In this paper we present a model to estimate the amplifier performance of various fiber designs, including complex microstructured designs. The semi-analytic approach in [8,9] is extended and the TMI threshold is estimated. The previous limitation of constant mode profiles in the semi-analytic model is addressed by using mode profiles that depend on thermal load. Analytic considerations for thermally induced mode coupling are combined with mode distributions found by finite element modesolvers (FEM), which ensures low computational time, on the order of minutes per thermal load (standard PC). Potentially, this model can be extended to consider other rare-earth materials, include system dependent properties such as specific noise frequency components, or include altering mode profiles along the fiber. We apply the model to a distributed modal filtering rod fiber (DMF85) with a core diameter of 85 μm [2].

2. Thermally induced waveguide perturbation and mode distributions

Operating temperatures of fiber amplifiers increase with increasing extracted output power per unit length. The heat originates from the energy difference between pump and signal photons i.e. the quantum defect, and dissipates from the active core towards the fiber boundary, yielding a temperature gradient over the fiber cross section. Rod fiber amplifiers are double clad structures having an outer air cladding guiding high NA pump light. The temperature gradient within the air cladding affects all allowed modes, and perturbs the waveguiding properties especially for core guided modes. The guided mode properties and the thermo-optic coupling between different guided modes are mainly determined by the temperature profile in the core region, which is not significantly affected by the presence of an air cladding. Temperatures on the order of 100°C – 200°C are reached within the air cladding causing significant increments in the refractive indices for large core low NA fibers.

For the purpose of calculating temperature profiles, the PCF structure of the rod fiber is approximated by a set of four concentric cylindrical layers [10], corresponding to the core,

#189034 - $15.00 USD Received 17 Apr 2013; revised 13 Jun 2013; accepted 13 Jun 2013; published 20 Jun 2013

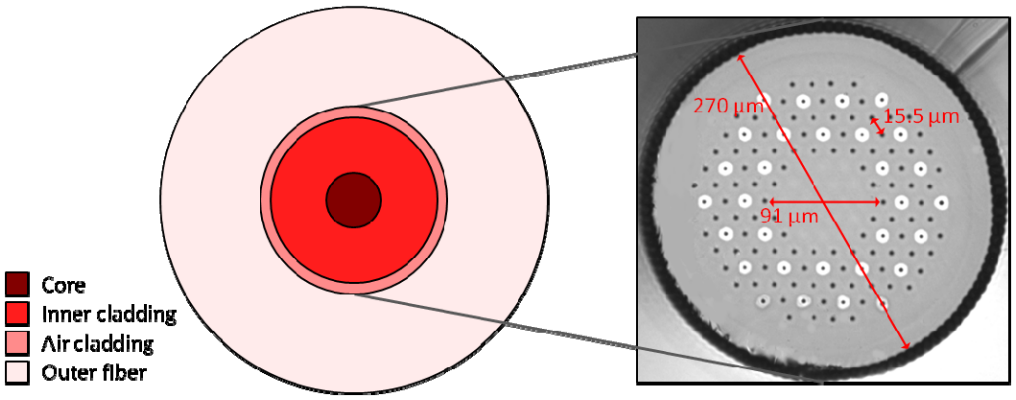

Fig. 1. The rod fiber cross section (right) is approximated by four concentric circles representing core, inner cladding, air cladding, and outer fiber (left). The heat load Q_0 is assumed uniform across the core.

inner cladding, air cladding, and outer fiber, see Fig. 1. The radius of the core is given by the area of the gain medium in the rod fiber amplifier.

The heat gradient is much larger in the radial cross section than along the fiber length, thus for an isotropic medium the steady state heat equation is [11]

$$\frac{1}{r}\frac{\partial}{\partial r}\left(r\frac{\partial T(r)}{\partial r}\right)=-\frac{q}{k_i}, \tag{1}$$

where the heat load density q is the heat load Q divided by the area of the active core A_{core}. Q is Q_0 in the core and 0 outside the core, and k_i is the thermal conductivity of the i'th layer. The parameters used in the calculations are given in Table 1.

The heat load generated in the gain medium depends on the quantum defect and increases with pump, P_{pump} [12]. The slope efficiency S of the rod fiber is included as a reasonable approximation for determining the heat load as a function of signal power, P_{signal}.

$$Q_0=\frac{1-10^{-\alpha dL/10}}{dL}\left(1-\frac{\lambda_p}{\lambda_s}\right)P_{pump}\simeq\frac{1-10^{-\alpha dL/10}}{dL}\left(1-\frac{\lambda_p}{\lambda_s}\right)\frac{P_{signal}}{S}, \tag{2}$$

where α is the pump absorption, λ_p and λ_s is the pump and signal wavelength.

Table 1. Parameters used in this work

Parameter	Symbol	Value
Thermal conductivity for silica	k	1.38 W/(mK)
Thermal conductivity for air	k	0.023 W/(mK)
Pump absorption	α	10 dB/m
Pump wavelength	λ_p	976 nm
Signal wavelength	λ_s	1040 nm
Length of interest	dL	10 cm
Surrounding temperature	T_0	25° C
Slope efficiency	S	70%
Heat flow coefficient	h	500 W/(m^{2}K)
Thermo-optic coefficient	η	3.5×10^{-5} K^{-1}
Density and specific heat capacity	ρC	1.67×10^{6} J/(Km^3)
Seed power	P_{seed}	10 W
Initial HOM content	ξ_{in}	0.05
Relative intensity noise	R_N	−100 dBc/Hz, −120 dBc/Hz

#189034 - $15.00 USD Received 17 Apr 2013; revised 13 Jun 2013; accepted 13 Jun 2013; published 20 Jun 2013

The fraction describes the change in pump power within dL due to pump photons converted to signal photons, and the bracket is the quantum defect for the pump photons. The largest heat load is assumed at the fiber output end in a backwards pumped configuration, where the rod fiber attains the highest stimulated emission and thereby largest quantum defect heating. Hence the last 10 cm of the rod fiber dL is considered for estimating the generated heat load as a function of signal power. The slope efficiency has been measured to 71% – 75% for the DMF85, and is set to 70% in the calculations. The thermal load, and therefore the threshold, for onset of TMI, depends on pump absorption. The small signal pump absorption is typically 20 dB/m for a rod fiber amplifier, but it decreases with increased population of the lasing level. The pump absorption is set to the realistic value of 10 dB/m in the calculations.

Heat diffusion is often compared to electrical charge diffusion and can be thought of as heat flow through a thermal resistance. The solution in one layer of the fiber depends on the boundary condition of the surrounding layer. Inside the core the solution to Eq. (1) is parabolic, when assuming a uniform heat load over the gain medium

$$T(r) = T_{core} + \frac{Q_0}{4 A_{core} k_i}\left(r_{core}^2 - r^2\right), \tag{3}$$

T_{core} is the temperature at the core edge, and r_{core} is the core radius. The solution decays logarithmic outside the active material, where $Q = 0$ in Eq. (1).

$$T(r) = T_i + \frac{Q_0}{2\pi k_i}\ln\left(\frac{r_i}{r}\right) \tag{4}$$

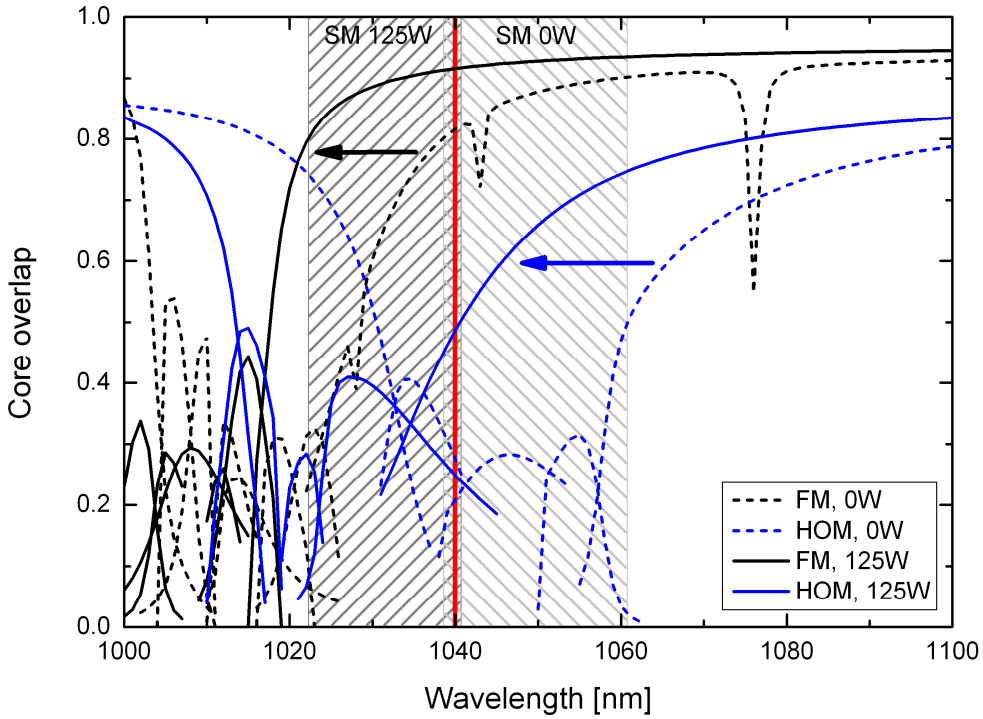

Fig. 2. Core overlap as a function of wavelength calculated for a cold DMF rod fiber and at a heat load corresponding to 125 W of extracted output power. The SM region is shaded and the signal wavelength at 1040 nm is marked by the red line. The increased heat load slightly blueshifts the curves indicated with the arrows.

#189034 - $15.00 USD Received 17 Apr 2013; revised 13 Jun 2013; accepted 13 Jun 2013; published 20 Jun 2013

i represents the current layer, thus T_i is the temperature at the outer boundary, and r_i is the outer radius of layer i. The air cladding is thin silica bridges separating air holes, and is approximated by an effective thermal conductivity given by the number of air holes, the air clad width and the width of the silica bridges separating the air holes [13]. The fibers are assumed to be placed in water at temperature T_0 with forced convective cooling with coefficient h, yielding a temperature at the fiber edge of

$$T_{fiber\ edge} = T_0 + \frac{Q_0}{2\pi r_{fiber} h} \tag{5}$$

The temperature increase of the fiber causes a refractive index increase across the entire fiber cross section due to the thermo-optic effect with coefficient η.

$$\Delta\varepsilon = \eta\left(T(r) - T_0\right) \tag{6}$$

The numerically estimated waveguide perturbations are used in mode calculations to find the transverse mode distribution. The fiber cross section, Fig. 1 (right), is modeled with the commercially available software package COMSOL Multiphysics® using the FEM [14]. The DMF85 rod fiber is a distributed modal filtering fiber and filters out HOMs from the core to the cladding in a specific spectral range, where the rod fiber is effectively SM. Figure 2 shows the core overlap as a function of wavelength for a cold DMF rod fiber and at a heat load corresponding to 125 W of signal power. The simulated cold DMF85 rod fiber is estimated to be SM from 1039 nm to 1060 nm based on a criterion of minimum 80% FM core overlap and maximum 50% HOM core overlap [15]. Thus the FM is well guided and the majority of the HOM is distributed outside the core. The SM region blueshifts with increasing heat load as indicated with the shaded regions in Fig. 2. However, the resonant cladding structure also

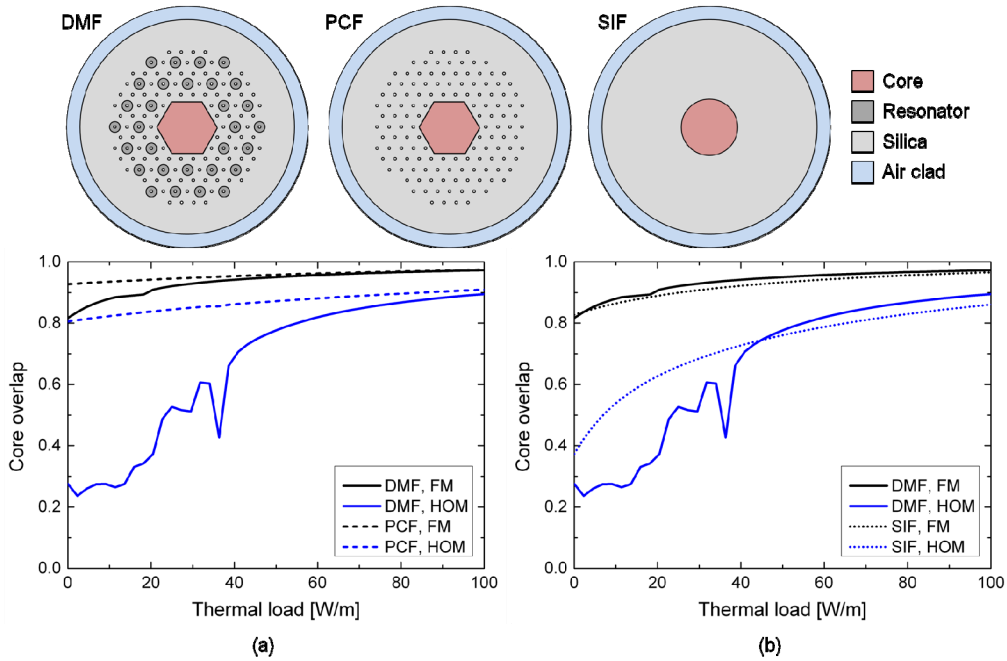

Fig. 3. Core overlap as a function of thermal load at signal wavelength of 1040 nm showing decreasing differential mode overlap with increasing thermal load. (a) Comparing DMF85 rod fiber with a 19 cell core PCF having the same structure as the DMF85 rod fiber without the resonators. (b) Comparing DMF85 rod fiber with a single mode SIF having $V = 2.40$.

#189034 - $15.00 USD Received 17 Apr 2013; revised 13 Jun 2013; accepted 13 Jun 2013; published 20 Jun 2013

experiences a heat load and insures SM properties of the DMF rod fiber for large heat loads [10]. The core overlap as a function of heat load for the DMF85 rod fiber is compared to a 19cell core PCF, whose cross section is equal to the DMF rod fiber without the resonator inclusions in Fig. 3(a). Core overlap is calculated within the hexagonal area of the DMF85 rod fiber and PCF i.e. the active region. The PCF is multi mode (MM) for this fiber structure, and has a large FM and HOM core overlap. Thus the DMF85 would be MM without the resonators. The DMF resonant cladding structure insures a low HOM core overlap within the SM regime and thereby high differential mode overlap. The increasing heat load increases the core cladding index step causing the guiding properties of the DMF rod fiber to approach the ones of the PCF, as the DMF85 is operated in the MM regime.

In Fig. 3(b) the DMF85 rod fiber is compared to a SM step index fiber (SIF) with 35 μm core radius and core cladding index step of 4.4×10^{-5}, smaller than technologically feasible, yielding an NA of 0.011 and $V = 2.40$. The SIF core area is equal to the doped area of the DMF and PCF. The SIF SM properties suffer from increasing heat load causing the HOM core overlap to increase significantly making the fiber MM at $Q = 7$ W/m, where the HOM content is larger than 50%. The DMF rod fiber experiences larger differential mode overlap within the SM regime compared to the SM SIF, indicating that the intentional HOM delocalization by the resonator elements in the cladding efficiently suppress HOM content in the core. The DMF85 rod fiber can tolerate a heat load up to $Q = 24$ W/m, before the HOM content increases above 50%. This shows that the modal stability of this resonant structure is significantly more robust than in the SIF. The thermally induced waveguide perturbations also affect the mode field diameter (MFD) of the FM, since increasing thermal load yields larger core confinement, see Fig. 4, and is estimated to a linear decrease in MFD of 2% per 100 W of extracted output power for DMF85.

Figure 5 shows the calculated mode distributions of the FM and first HOM for increasing signal powers. The thermal load increases the core refractive index and slowly blueshifts the SM window of the DMF85 for increasing signal power [16]. At some core temperature the MM regime has shifted to the signal wavelength, and the first HOM becomes guided with increasing core overlap, eventually causing TMI.

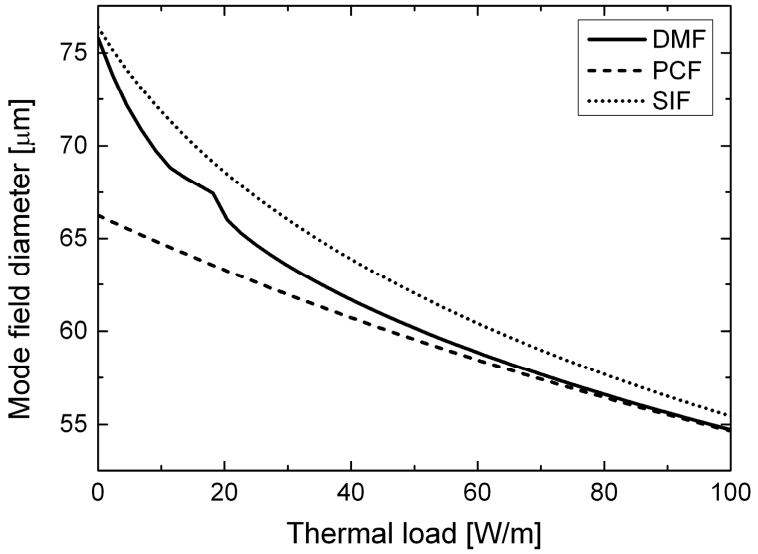

Fig. 4. Mode field diameter as a function of thermal load.

#189034 - $15.00 USD Received 17 Apr 2013; revised 13 Jun 2013; accepted 13 Jun 2013; published 20 Jun 2013

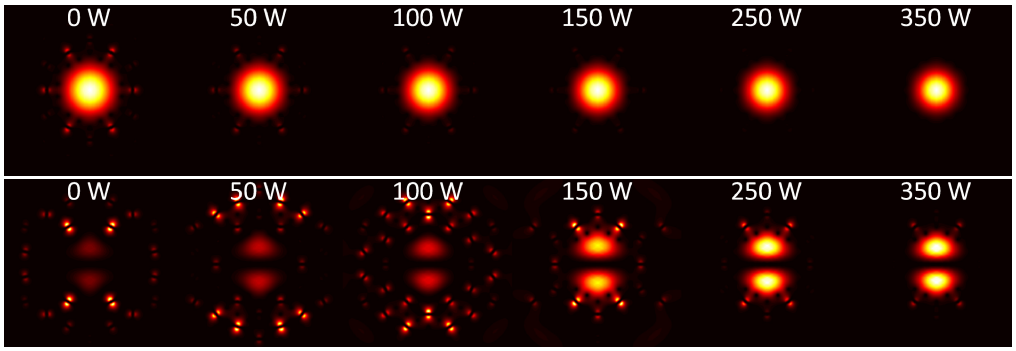

Fig. 5. Calculated mode distributions of the FM (top) and first HOM (bottom) for the DMF85 rod fiber for selected signal powers. Larger thermal load causes larger core confinement.

3. Estimating modal instability threshold

The semi-analytic model by Hansen et *al.* [8,9], describing TMI in fiber amplifiers is combined with FEM calculations to estimate the TMI threshold for PCF fibers. The mode power transfer is determined by a nonlinear coupling constant χ that depends on the frequency difference Ω between the FM and HOM, the bulk gain coefficient g, and the transverse core overlap ratio Γ of the FM and HOM determined from the mode calculations. The nonlinear coupling constant χ is given by [8,9]

$$\chi(\Omega) = \frac{\eta\omega^2}{k_{fiber}\beta c^2}\,\mathrm{Im}\left[A(\Omega)\right]\left(1-\frac{\lambda_s}{\lambda_p}\right) \tag{7}$$

where η is the thermo-optic coefficient and β is the propagation constant. A is an effective overlap integral that is determined from the mode distributions ψ for the FM and HOM

$$A(\Omega) = \iint \psi_{FM}(r_\perp)\psi_{HOM}(r_\perp)\iint_{core} G(r_\perp, r_\perp', \Omega)\psi_{FM}(r_\perp')\psi_{HOM}(r_\perp')\mathrm{d}^2 r_\perp' \mathrm{d}^2 r_\perp \tag{8}$$

The inner integral is over the doped core region, and the outer integral is over the full cross section for the transverse coordinates $r_\perp'$ and $r_\perp$. The Green's function G is the solution to the Fourier transformed transient heat equation that describes the change in temperature due to the thermal load Q. Assuming G to be translation invariant it is given by

$$G(r_\perp - r_\perp', \Omega) = \frac{1}{2\pi} K_0\left[\sqrt{\frac{i\rho C}{k}\Omega}\,(r_\perp - r_\perp')\right], \tag{9}$$

where K_0 is the zeroth order modified Bessel function of second kind, ρ is the density, and C is the specific heat capacity. G is a convolution operator that allows the inner integral in Eq. (8) to be determined by the convolution theorem. χ in Eq. (7) is an odd function that tends towards zero as Ω approaches zero. Therefore, there must be a seed to initialize power transfer from the FM to the HOM. We consider TMI seeded by relative intensity noise (RIN) R_N from the seed laser. The approximate expression for the fraction of HOM power content ξ_{out} as a function of extracted average output power P_{signal} is given by [9]

$$\xi_{out} = \xi_{in}\left(\frac{P_{seed}}{P_{signal}}\right)^{1-\frac{\Gamma_{HOM}}{\Gamma_{FM}}}\left(1+\frac{1}{4}R_N\sqrt{\frac{2\pi\Gamma_{FM}}{\left|\chi''(\Omega_p)\right|P_{signal}}}\exp\left[\frac{\chi(\Omega_p)}{\Gamma_{FM}}\left(P_{signal}-P_{seed}\right)\right]\right) \tag{10}$$

#189034 - $15.00 USD Received 17 Apr 2013; revised 13 Jun 2013; accepted 13 Jun 2013; published 20 Jun 2013

where P_{seed} is the seed power and Ω_p is Ω for maximum χ, and ξ_{in} is the fraction of power that is initially coupled to the HOM. A seed laser is characterized by its RIN, which can be on the order of −120 dBc/Hz to −100 dBc/Hz corresponding to a laser with low and high RIN.

The HOM content vs. output power increases abruptly at the TMI threshold and 10% HOM content is used in the calculations to define the TMI threshold. Figure 6 shows the calculated TMI threshold as a function of thermal load using Eq. (10). The solid and dashed curves are calculated for R_N = −120 dBc/Hz and R_N = −100 dBc/Hz, and represent a TMI threshold interval depending on RIN. The DMF85 rod fiber is initially SM at the signal wavelength with the SM window slightly blueshifting as the fiber heats up, and the HOM becomes guided at high thermal loads corresponding to high extracted output power. The thermal load is proportional to signal power, therefore the estimated TMI threshold occurs when the calculated TMI threshold matches the signal power used in the thermal load calculations. This happens at 371 W and 443 W, as indicated in Fig. 6. For comparison the TMI threshold of the PCF and theoretical SIF in Fig. 3(a) and Fig. 3(b) are estimated to 348 W – 426 W and 392 W – 470 W for R_N = −100 dBc/Hz – R_N = −120 dBc/Hz respectively. This is slightly higher for the PCF and slightly lower for the SIF compared to the DMF85, as expected based on the differential mode overlap in Fig. 3. The SM window of the DMF85 can be shifted by changing the designs parameters, which allow engineering the DMF85 rod fiber to have SM operation at high or low signal power depending on the application [15].

The TMI threshold for the DMF rod fiber has been measured to 292 W [16], which is lower than the estimated threshold. However it is comparable and the deviation is assumed to

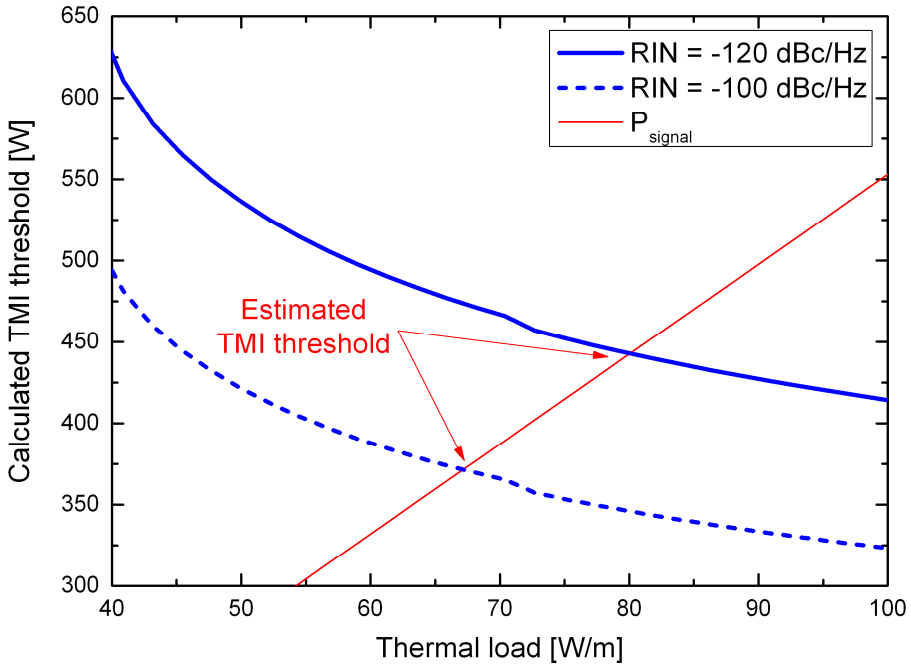

Fig. 6. Calculated TMI threshold as a function of thermal load using two values of RIN −120 dBc/Hz (solid) and −100 dBc/Hz (dashed) representing a seed laser with low and high RIN. The crossing of signal power vs. thermal load indicates the estimated TMI threshold for the DMF85 rod fiber.

be model dependent and not fiber design dependent, which allows the use of this model as a manufacturing tool for comparing various fiber designs.

Several system dependent parameters can be speculated to influence the estimated TMI threshold. Recent studies have also showed large dependency between TMI threshold and system parameters such as seed or pump noise as well as cooling conditions [6,19]. Seed

#189034 - $15.00 USD Received 17 Apr 2013; revised 13 Jun 2013; accepted 13 Jun 2013; published 20 Jun 2013

noise can contain discrete frequency components possibly larger than the RIN, that if located within the frequency band of the nonlinear coupling constant reduces the TMI threshold. Any system induced loss such as photodarkening would increase the heat load and lower the TMI threshold as a function of operation time. This causes an initially stable output to become unstable as PD losses increase over time. The ability to support the HOM is highly dependent on small core refractive index changes, which could also explain a part of the deviation between calculations and measurement. It is also assumed in the calculations that the density, heat capacity, thermal conductivity, and thermo-optic coefficient are temperature independent. In experiments, the absolute temperature of the fiber increases significantly at high output power [6] and depends on outer cooling properties, which can lead to variations in these coefficients.

4. Conclusion

We have expanded a semi-analytic model to include calculations on complex microstrutered fibers with thermally induced waveguide perturbations to estimate the TMI threshold for ytterbium doped rod fiber amplifiers. The change in refractive index due to the quantum defect heating was calculated from the thermal load and used in FEM calculations to achieve mode distributions, which were combined with a semi-analytic model to estimate the TMI threshold. The DMF85 rod fiber was considered as an example with estimated TMI threshold of 371 W – 443 W, slightly higher than a previously measured TMI threshold. We believe that the presented model can be used as a manufacturing tool for comparing rod fiber performance.

#189034 - $15.00 USD Received 17 Apr 2013; revised 13 Jun 2013; accepted 13 Jun 2013; published 20 Jun 2013